

# Recrystallization of atomically balanced amorphous pockets in Si: A source of point defects

Luis A. Marqués,\* Lourdes Pelaz, Pedro López, Iván Santos, and María Aboy

*Departamento de Electrónica, Universidad de Valladolid, E.T.S.I. de Telecomunicación, 47011 Valladolid, Spain*

(Received 3 September 2007; published 24 October 2007)

We use classical molecular dynamics simulation techniques to study the regrowth behavior of amorphous pockets in Si. We demonstrate that crystallization depends on the morphology of the pocket-crystal interface. Although our simulated amorphous pockets had not any excess nor deficit of atoms with respect to perfect crystal, after regrowth we found residual defects. Most of them are single Si interstitials and vacancies, but also larger defects have been encountered. We have determined their atomic structures and calculated their formation energies. These complexes are more stable than amorphous pockets, and may trigger the formation of extended defects or favor damage accumulation.

DOI: [10.1103/PhysRevB.76.153201](https://doi.org/10.1103/PhysRevB.76.153201)

PACS number(s): 61.72.Cc, 61.43.Dq, 61.82.Fk, 64.60.Cn

## I. INTRODUCTION

Since the beginning of the use of ion implantation for the fabrication of Si devices, ion-beam-induced amorphization and solid-phase epitaxial regrowth (SPER) in Si have been the subject of a great number of studies (for a recent review see Ref. 1). There is now a renewed interest in the modeling of these processes because of their technological relevance for the semiconductor industry. The collision cascade initiated by the incoming ion causes the formation of Si interstitial ( $I$ ) and vacancy ( $V$ ) defects, and also amorphous pockets ( $a$  pockets) by local melting of regions where enough energy is deposited.<sup>2-6</sup> In spite of the complexity and particular morphology of each collision cascade, the net atomic balance is null (except by a generally small sputtering contribution) and only the introduced ion leads to an excess atom within the lattice.<sup>7</sup> Nevertheless, the momentum transfer of the energetic ion causes some spatial separation between the recoil atoms ( $I$  defects) and the empty lattice sites ( $V$  defects) they leave behind, which can make their recombination difficult.<sup>8</sup> It is important to determine the effectiveness of damage recombination because residual defects affect dopant diffusion and activation which, in turn, modify the junction profiles and device characteristics.<sup>9</sup> Defects also cause carrier mobility degradation and increase leakage currents.

It is generally assumed that when  $I$  and  $V$  defects are within the interaction radius of each other, they recombine instantaneously. However, tight-binding calculations show that instead a metastable defect known as  $IV$  pair or bond defect (BD) is formed.<sup>10,11</sup> Although its lifetime is very short, we demonstrated in a previous paper that accumulation of these defects can lead to local amorphization of the Si lattice.<sup>12</sup> The regrowth of amorphous regions is well defined for the case of planar amorphous-crystal interfaces,<sup>13,14</sup> but many questions remain open for the regrowth of isolated  $a$  pockets. Experiments on the regrowth of isolated  $a$  pockets produced in Si by Xe ion implantation show a dependence on pocket size.<sup>2</sup> This has also been observed in molecular dynamics (MD) simulations,<sup>3</sup> where larger pockets have greater metastability against recrystallization. However, Donnelly *et al.* studied the regrowth behavior of  $a$  pockets also created by Xe implantation into Si, observing that pockets of similar sizes had completely different recrystallization rates.<sup>4</sup>

In this paper we present classical MD simulation experiments specifically designed to determine the mechanism that governs the regrowth behavior of  $a$  pockets in Si. Our results will be interpreted in terms of proposed atomistic models for amorphization and recrystallization in Si.<sup>15</sup> We also analyze the residual damage which is obtained after regrowth of atomically balanced  $a$  pockets.

## II. MD SIMULATION DETAILS

We have used systems consisting of 6084 Si atoms in a computational MD cell whose dimensions were  $9a \times 13\sqrt{2}a \times 13\sqrt{2}a$ , being  $a$  the basic unit length of the Si diamond lattice (5.43 Å). The cell was bounded by two (100) planes in the  $X$  direction and by four (110) planes in  $Y$  and  $Z$  directions. To minimize finite size effects we used periodic boundary conditions along the three axes. We have chosen the Tersoff 3 potential to describe the atomic interactions<sup>16</sup> since it has been shown to reproduce fairly well the structural properties of point defects<sup>17,18</sup> and the amorphous phase.<sup>19</sup> Equations of motion were integrated using the fourth order Gear predictor-corrector algorithm.<sup>20</sup>

We have generated  $a$  pockets in our MD cell by introducing BDs. The BD consists of a local rearrangement of bonds with no excess or deficit of atoms (see Fig. 1). Although atoms remain fourfold coordinated, the BD introduces disorder in the lattice since two atoms are displaced with respect to perfect lattice positions, and five- and seven-membered rings typical of the amorphous phase are created.<sup>12</sup> This method of introducing damage in the Si lattice is similar to the algorithm developed by Wooten, Winer, and Weaire,<sup>21</sup> although the atomic displacements are somewhat different. We have generated two types of  $a$  pockets in the center of our MD cell by introducing a total of 510 BDs, in one case arranged within a sphere (diameter of 3.4 nm) and in the other one within a cube (side of 2.7 nm). These sizes correspond to the same volume in the Si lattice, and are typical dimensions of  $a$  pockets experimentally obtained by Xe ion irradiation of Si.<sup>4</sup> Both types of pockets were annealed at a temperature of 1400 K, as high as possible to accelerate system dynamics but staying below the melting temperature of the Si amorphous phase predicted by the Tersoff 3 potential.<sup>22</sup> During  $a$  pocket crystallization, energy was freed

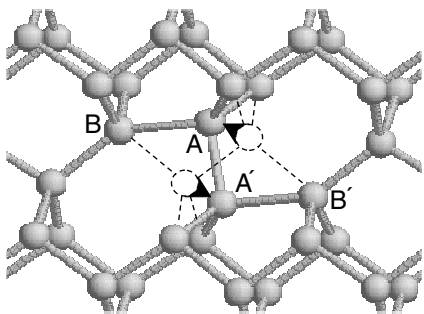


FIG. 1. Atomic structure of the bond defect. Dashed lines represent atoms and bonds in the perfect lattice. The bond defect is formed when atoms  $A$  and  $A'$  move along the directions indicated by the arrows, switching bonds with atoms  $B$  and  $B'$ . Their reverse movement represents an elementary crystallization event.

in the form of latent heat. To avoid an artificial temperature increase due to periodic boundary conditions, atom velocities were rescaled every 1000 time steps to maintain 1400 K in the cell. To improve statistics, each  $a$  pocket annealing simulation was repeated twenty times varying the initial atomic velocity distribution. With these simulation experiments we have made a comparative study of the crystallization behavior of  $a$ -pocket structures of the same size but with different arrangement of the crystal-amorphous interface.

We have measured  $a$ -pocket annealing times by monitoring the number of “amorphous atoms” within the MD cell. To do so we have used a method based on the time average of the atom coordinates, which has been successfully used to study recrystallization processes in Si,<sup>3,23</sup> and the configurational and energetic properties of the Si self-interstitial.<sup>18</sup> Atomic cell configurations are averaged in time during 1000 time steps. In this way it is possible to eliminate thermal vibrations and consequently to obtain clean configurations that can be compared to the perfect lattice at 0 K. When an atom in the averaged configuration is closer than  $0.7 \text{ \AA}$  to a lattice site the atom is associated to that site, otherwise it is labeled as amorphous. For example, in a MD cell with a single BD this method identifies two amorphous atoms (the two displaced atoms that the BD has with respect to perfect crystal,  $A$  and  $A'$  in Fig. 1). Since crystallization is incomplete in some simulations (as we shall explain later), we have defined the  $a$ -pocket annealing time when the total number of amorphous atoms within the MD cell is lower than 5% the initial value (approximately 50 atoms).

### III. RESULTS AND DISCUSSION

Average annealing times obtained for amorphous spheres and cubes are  $623 \pm 31$  ps and  $500 \pm 30$  ps, respectively. Amorphous cubes regrow on average 25% faster than amorphous spheres, in spite of having the same number of initial amorphous atoms. To illustrate the annealing behavior, in Fig. 2 we show the number of amorphous atoms as a function of time for two representative cases. The cube regrowth is characterized by a faster decay in the number of amorphous atoms with respect to the sphere regrowth. In both cases, there is a final fast decay when the  $a$ -pocket size reach

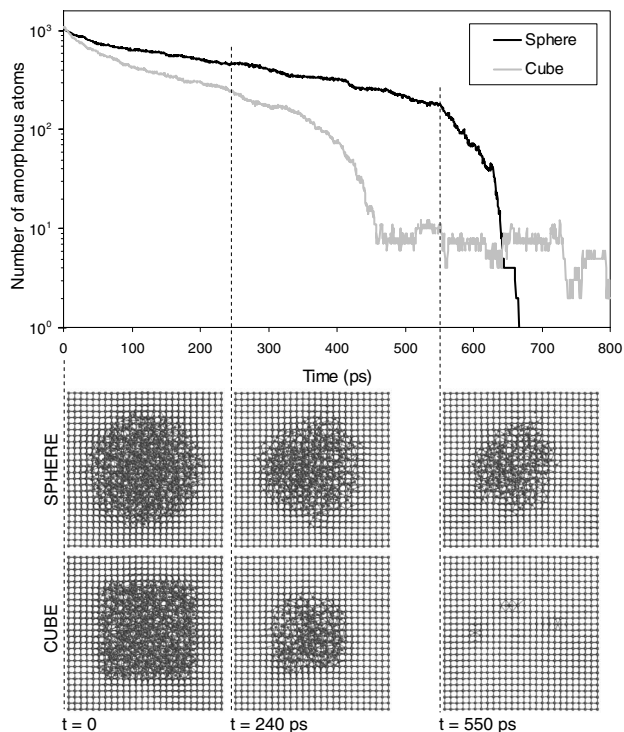


FIG. 2. Number of amorphous atoms as a function of time for two representative simulations of amorphous sphere and cube annealings at 1400 K. Below YZ projections of the MD cell taken at the indicated times are shown.

a value close to 100. In the particular case of the amorphous cube shown here, some residual damage remains in the lattice after annealing.

Figure 2 also shows several snapshots which illustrate the atomic evolution of the representative sphere- and cube-shaped  $a$  pockets during their annealing. In both cases crystallization starts from the crystal-amorphous interface. The faster decay in the number of amorphous atoms in the cube is associated to the regrowth of its vertexes and edges. After 240 ps of annealing, the cubical  $a$  pocket has adopted a more spherical shape. Its crystallization continues at a faster pace than the initially spherical  $a$  pocket. MD studies on the recrystallization kinetics of  $a$  pockets directly created by heavy-ion irradiation in Si also indicate that regrowth starts preferentially at their protruding zones and that it occurs without the intervention of external defects.<sup>3</sup>

Our MD results show that crystallization of  $a$  pockets depends on the amorphous-crystal interface morphology. Such finding explains experimental observations where  $a$  pockets of similar sizes have very different annealing behavior.<sup>4</sup> This is consistent with amorphization and recrystallization models which assume that activation energy for BD recombination increases with the number of surrounding BDs: a BD is less stable when it has a lower number of neighboring BDs.<sup>15</sup> Thus, vertexes and edges of the cube recombine quickly corresponding to BDs surrounded by less neighboring BDs. The influence of  $a$ -pocket size on stability reported by some authors<sup>2,3</sup> arises indirectly through differences on amorphous-crystal interface curvatures. Smaller  $a$  pockets recombine faster because BDs lying on the

amorphous-crystal interface have less BD neighbors and thus are less stable.

An interesting result extracted from the analysis of the regrowth kinetics of these atomically balanced  $a$  pockets is that the final number of amorphous atoms is not always zero, as it can be seen in Fig. 2 for the case of the cubical  $a$ -pocket annealing. The corresponding snapshot shows some residual defects remaining in the lattice after crystallization. Although we have chosen this particular simulation to illustrate this observation, we have confirmed that the persistence of post-crystallization damage is relatively frequent. It happened in 35% of the sphere simulations and in 55% of the cube simulations. This may seem, in principle, an unexpected result since in our simulations  $a$  pockets have been created by accumulation of BDs and there is no excess or deficit of atoms with respect to perfect crystal. In all simulations where residual damage is obtained, each  $I$  defect (or defects) is compensated by the corresponding  $V$  defect (or defects). Their spatial separation prevented complete defect recombination.

The formation of residual defects when the initial  $a$ -pocket has the same density than perfect crystal is a consequence of the higher free energy content of the amorphous phase.<sup>24</sup> Upon crystallization, amorphous atoms near the amorphous-crystal interface move to sites consistent with the perfect lattice and regrow. The surrounding atoms in the amorphous phase rearrange to find an equivalent or lower energy state with a different atomic configuration. Sometimes, this atomic rearrangement leads to local density fluctuations and consequently to the formation of separated defects as crystallization proceeds. In fact, using MD it has been observed that recrystallization of  $a$  pockets directly created by irradiation frees point defects to the lattice, being its number not always correlated to the density fluctuations these  $a$  pockets show with respect to perfect crystal.<sup>3,5</sup> Similar interface effects that lead to residual defects (in the form of divacancies, stacking faults, twins, interstitial loops, etc.) upon crystallization have been observed in MD simulations of crystal growth from the liquid phase in Si and SiC.<sup>14,23,25–27</sup>

The formation of residual defects is more likely to happen in large pockets with elongated shapes and protruding zones, because these may become isolated as crystallization proceeds. Any local excess or deficit of atoms with respect to perfect crystal will give rise to some residual damage in the lattice. This explains why, on average, there are more residual defects after crystallization of amorphous cubes. From this reasoning, it would be expected a smaller percentage of residual damage generation for smaller pockets. To confirm this, we carried out annealing simulations at 1400 K of amorphous spheres and cubes of a smaller size, 400 BDs, obtaining also residual damage but with less frequent occurrences, of 25% in both pocket type simulations. At this smaller size these two pocket types behave as compact structures with respect to annealing. It is worth to note that in our simulations the generation of defects during  $a$ -pocket annealing neither precluded further crystallization, nor significantly affected crystallization rates.

The analysis of the defects spontaneously arising from the incomplete annealing of  $a$  pockets indicates that most of them are single self-interstitials and vacancies, diinterstitials

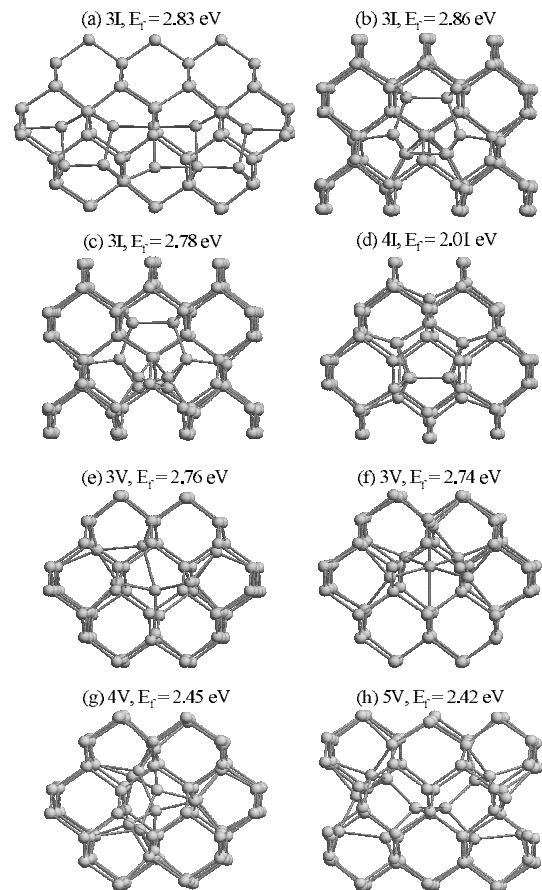


FIG. 3. Ball-and-stick models of residual defects obtained after annealing of  $a$  pockets. The formation energy per defect  $E_f$  is also indicated.

and divacancies (25% in the sphere and 35% in the cube simulations), but in some cases larger defects are formed. Defect complexity is not related to the initial  $a$ -pocket shape nor size since larger defects appear both in cube and sphere annealing simulations of 510 and 400 BDs. Relevant defect atomic configurations are represented in Fig. 3, along with the corresponding formation energy per defect  $E_f$ . We have found three different configurations for the tri-interstitial (3I). The first one, Fig. 3(a), is a combination of one tetrahedral and two extended interstitials,<sup>18</sup> which are all aligned along the  $[100]$  direction. This structure can grow longer by adding more tetrahedral and extended Si interstitials on both edges. Tri-interstitials shown in Figs. 3(b) and 3(c) are more compact structures where all atoms are fourfold coordinated. These last two configurations were found by Richie and Kim using a combination of tight-binding, *ab initio* and real-time multiresolution analysis techniques.<sup>28</sup> They found formation energies per defect of 2.8 and 2.1 eV, respectively, in very good agreement with our results. The defect in Fig. 3(d) is a tetrainterstitial (4I), where all atoms are also fourfold coordinated. This defect has also been studied by means of tight-binding and *ab initio* techniques,<sup>29–31</sup> and a formation energy between 1.5 and 2.1 eV was found. It is believed to be related to the experimentally measured B3 center in irradiated Si,<sup>30</sup> and also that it acts as nucleation center for extended

{113} defects.<sup>31</sup> As for the vacancy defects, configurations obtained from our simulations are shown in Figs. 3(e)–3(h) for the case of two trivacancies (3V), a tetravacancy (4V), and a pentavacancy (5V). All of them are highly symmetrical configurations, and are characterized by large atomic rearrangements with respect to the perfect Si lattice. Although not identical, they show very strong similarities with the configurations obtained by Makhov and Lewis using density-functional-theory calculations, especially regarding the atom rearrangements along five-member rings.<sup>32</sup> Formation energies are also in fair agreement. In particular, the tri-vacancy of Fig. 3(e) has been also observed by Ishimaru *et al.* in their MD simulations of Si crystal growth from the melt.<sup>13</sup> Small point defects, single interstitials up to tri-interstitials, single vacancies, and divacancies, are highly mobile species and diffuse fast through the Si lattice.<sup>33,34</sup> More complex defect clusters are immobile. Mobile defects may diffuse around until they recombine, interact with dopants, or are trapped by more complex and immobile clusters. These defects, more stable than *a* pockets, can also favor damage accumulation.

#### IV. CONCLUSIONS

We have used classical MD simulation techniques to study the annealing of *a* pockets in Si. We have demon-

strated that crystallization does not depend on pocket size, but on the morphology of the pocket-crystal interface. We found that *a* pockets can be the origin of point defects even when they have no excess nor deficit of atoms with respect to perfect crystal. We have analyzed their atomic structures and calculated their formation energies, showing a very good agreement with results obtained by other authors using more fundamental simulation techniques. It is important to note that, while in those fundamental simulations defect structures were inferred mainly by geometrical considerations, in our simulations they are obtained spontaneously as the result of the own crystallization dynamics. The generation of immobile Si interstitial clusters, such as the highly stable tetrainterstitial, can ultimately trigger the formation of extended {113} defects or act as preferential sites for damage accumulation and lattice amorphization.

#### ACKNOWLEDGMENTS

This work has been supported by the Spanish DGI under Project No. TEC2005-05101 and the JCyL Consejería de Educación y Cultura under Project No. VA070A05.

\*lmarques@ele.uva.es

<sup>1</sup>L. Pelaz, L. A. Marqués, and J. Barbolla, *J. Appl. Phys.* **96**, 5947 (2004).

<sup>2</sup>I. M. Robertson and I. Jenčič, *J. Nucl. Mater.* **239**, 273 (1996).

<sup>3</sup>M.-J. Caturla, T. Diaz de la Rubia, L. A. Marqués, and G. H. Gilmer, *Phys. Rev. B* **54**, 16683 (1996).

<sup>4</sup>S. E. Donnelly, R. C. Birtcher, V. M. Vishnyakov, and G. Carter, *Appl. Phys. Lett.* **82**, 1860 (2003).

<sup>5</sup>T. Diaz de la Rubia and G. H. Gilmer, *Phys. Rev. Lett.* **74**, 2507 (1995).

<sup>6</sup>I. Santos, L. A. Marqués, and L. Pelaz, *Phys. Rev. B* **74**, 174115 (2006).

<sup>7</sup>M. Jaraiz, G. H. Gilmer, J. M. Poate, and T. D. de la Rubia, *Appl. Phys. Lett.* **68**, 409 (1996).

<sup>8</sup>L. Pelaz, G. H. Gilmer, M. Jaraiz, S. B. Herner, H.-J. Gossmann, D. J. Eaglesham, G. Hobler, C. S. Rafferty, and J. Barbolla, *Appl. Phys. Lett.* **73**, 1421 (1998).

<sup>9</sup>N. E. B. Cowern, G. Mannino, P. A. Stolk, F. Roozeboom, H. G. A. Huizing, J. G. M. van Berkum, F. Cristiano, A. Claverie, and M. Jaraiz, *Phys. Rev. Lett.* **82**, 4460 (1999).

<sup>10</sup>M. Tang, L. Colombo, J. Zhu, and T. Diaz de la Rubia, *Phys. Rev. B* **55**, 14279 (1997).

<sup>11</sup>S. Goedecker, T. Deutsch, and L. Billard, *Phys. Rev. Lett.* **88**, 235501 (2002).

<sup>12</sup>L. A. Marqués, L. Pelaz, J. Hernández, J. Barbolla, and G. H. Gilmer, *Phys. Rev. B* **64**, 045214 (2001).

<sup>13</sup>M. Ishimaru, S. Munetoh, T. Motooka, K. Moriguchi, and A. Shintani, *Phys. Rev. B* **58**, 12583 (1998).

<sup>14</sup>S. Munetoh, K. Moriguchi, A. Shintani, K. Nishihira, and T. Motooka, *Phys. Rev. B* **64**, 193314 (2001).

<sup>15</sup>L. A. Marqués, L. Pelaz, M. Aboy, L. Enríquez, and J. Barbolla, *Phys. Rev. Lett.* **91**, 135504 (2003).

<sup>16</sup>J. Tersoff, *Phys. Rev. B* **38**, 9902 (1988).

<sup>17</sup>P. J. Ungar, T. Halicioglu, and W. A. Tiller, *Phys. Rev. B* **50**,

7344 (1994).

<sup>18</sup>L. A. Marqués, L. Pelaz, P. Castrillo, and J. Barbolla, *Phys. Rev. B* **71**, 085204 (2005).

<sup>19</sup>M. Ishimaru, S. Munetoh, and T. Motooka, *Phys. Rev. B* **56**, 15133 (1997).

<sup>20</sup>C. W. Gear, *Numerical Initial Value Problems in Ordinary Differential Equations* (Prentice-Hall, Englewood Cliffs, NJ, 1971).

<sup>21</sup>F. Wooten, K. Winer, and D. Weaire, *Phys. Rev. Lett.* **54**, 1392 (1985).

<sup>22</sup>L. A. Marqués, L. Pelaz, M. Aboy, and J. Barbolla, *Nucl. Instrum. Methods Phys. Res. B* **216**, 57 (2004).

<sup>23</sup>L. A. Marqués, M.-J. Caturla, T. D. de la Rubia, and G. H. Gilmer, *J. Appl. Phys.* **80**, 6160 (1996).

<sup>24</sup>W. C. Sinke, A. Polman, S. Roorda, and P. A. Stolk, *Appl. Surf. Sci.* **43**, 128 (1989).

<sup>25</sup>F. Gao, Y. Zhang, M. Posselt, and W. J. Weber, *Phys. Rev. B* **74**, 104108 (2006).

<sup>26</sup>F. Gao, Y. Zhang, R. Devanathan, M. Posselt, and W. J. Weber, *Nucl. Instrum. Methods Phys. Res. B* **255**, 136 (2007).

<sup>27</sup>S. Izumi, S. Hara, T. Kumagai, and S. Sakai, *J. Cryst. Growth* **274**, 47 (2005).

<sup>28</sup>D. A. Richie, J. Kim, S. A. Barr, K. R. A. Hazzard, R. Hennig, and J. W. Wilkins, *Phys. Rev. Lett.* **92**, 045501 (2004).

<sup>29</sup>N. Arai, S. Takeda, and M. Kohyama, *Phys. Rev. Lett.* **78**, 4265 (1997).

<sup>30</sup>B. J. Coomer, J. P. Goss, R. Jones, S. Öberg, and P. R. Briddon, *J. Phys.: Condens. Matter* **13**, L1 (2001).

<sup>31</sup>M. Kohyama and S. Takeda, *Phys. Rev. B* **60**, 8075 (1999).

<sup>32</sup>D. V. Makhov and L. J. Lewis, *Phys. Rev. Lett.* **92**, 255504 (2004).

<sup>33</sup>S. K. Estreicher, M. Gharaibeh, P. A. Fedders, and P. Ordejón, *Phys. Rev. Lett.* **86**, 1247 (2001).

<sup>34</sup>G. S. Hwang and W. A. Goddard III, *Phys. Rev. B* **65**, 233205 (2002).